

# Improving performance of phase shift pulse BOTDR

Ryutaro Shibata<sup>a)</sup>, Hirofumi Kasahara, Lunider Paiva Elias,  
and Tsuneo Horiguchi

Graduate School of Engineering and Science, Shibaura Institute of Technology,  
3–7–5 Toyosu, Koto-ku, Tokyo 135–8548, Japan

a) [ma15048@shibaura-it.ac.jp](mailto:ma15048@shibaura-it.ac.jp)

**Abstract:** We propose a phase shift pulse BOTDR (PSP-BOTDR) using probes composed of long and short pulses with phase shift keying modulation, and evaluate its performance by experiment and simulation. Modifying the previous probe configuration reduces signal leakage from the adjacent section to a negligible extent, and achieves truly a spatial resolution of 20 cm.

**Keywords:** BOTDR, spontaneous Brillouin scattering, distributed fiber sensors

**Classification:** Optical systems

## References

- [1] K. Hotate and T. Hasegawa: “Measurement of Brillouin gain spectrum distribution along an optical fiber using a correlation-based technique: proposal, experiment and simulation,” *IEICE Trans. Electron.* **E83-C** (2000) 405.
- [2] Y. Mizuno, *et al.*: “One-end-access high-speed distributed strain measurement with 13-mm spatial resolution based on Brillouin optical correlation-domain reflectometry,” *IEEE Photonics Technol. Lett.* **21** (2009) 474 (DOI: [10.1109/LPT.2009.2013643](https://doi.org/10.1109/LPT.2009.2013643)).
- [3] T. Horiguchi, *et al.*: “A technique to measure distributed strain in optical fibers,” *IEEE Photonics Technol. Lett.* **2** (1990) 352 (DOI: [10.1109/68.54703](https://doi.org/10.1109/68.54703)).
- [4] T. Horiguchi, *et al.*: “Development of a distributed sensing technique using Brillouin scattering,” *J. Lightwave Technol.* **13** (1995) 1296 (DOI: [10.1109/50.400684](https://doi.org/10.1109/50.400684)).
- [5] C. H. Li, *et al.*: “PPP-BOTDA method to achieve cm-order spatial resolution in Brillouin distributed measuring technique,” *IEICE Tech. Rep.* **105** (2005) 1.
- [6] T. Horiguchi, *et al.*: “Negative Brillouin gain and its application to distributed fiber sensing,” *Proc. 33rd ECOC* (2007) P018 (DOI: [10.1049/ic:20070408](https://doi.org/10.1049/ic:20070408)).
- [7] H. Liang, *et al.*: “High-resolution DPP-BOTDA over 50 km LEAF using return-to-zero coded pulses,” *Opt. Lett.* **35** (2010) 1503 (DOI: [10.1364/OL.35.001503](https://doi.org/10.1364/OL.35.001503)).
- [8] Y. Koyamada, *et al.*: “Novel technique to improve spatial resolution in Brillouin optical time-domain reflectometry,” *IEEE Photonics Technol. Lett.* **19** (2007) 1910 (DOI: [10.1109/LPT.2007.908651](https://doi.org/10.1109/LPT.2007.908651)).
- [9] K. Nishiguchi, *et al.*: “Synthetic spectrum approach for Brillouin optical time-domain reflectometry,” *Sensors* **14** (2014) 4731 (DOI: [10.3390/s140304731](https://doi.org/10.3390/s140304731)).

- [10] R. Shibata, *et al.*: “Proposal and demonstration of high spatial resolution BOTDR by correlating signals sampled with narrow- and wide-width window functions,” Proc. 6th ICP (2016) 45 (DOI: [10.1109/ICP.2016.7510028](https://doi.org/10.1109/ICP.2016.7510028)).

## 1 Introduction

Optical fiber distributed sensor technology utilizing strain and temperature dependence of Brillouin frequency shift (BFS) in Brillouin scattering is expected to have applications in many fields such as health monitoring of large structures, and study has been actively conducted on improving its characteristics. Among them, the spatial resolution is one of the important capabilities of distributed sensors. Until now, its superior data such as 1.6 mm and 13 mm resolutions have been achieved by BOCDA (Brillouin Optical Correlation Domain Analysis) [1] and BOCDR (Brillouin Optical Correlation Domain Reflectometry) [2], respectively, where continuously modulated light is incident on optical fibers and Brillouin scattered light is measured in the optical correlation domain. In contrast, although BOTDA (Brillouin Optical Time Domain Analysis) [3] and BOTDR (Brillouin Optical Time Domain Reflectometry) [4], where pulse light is used and Brillouin scattered light is measured in the optical time domain, are excellent in the distance range of measurement, the spatial resolution remained about 1 m for a long time. However, BOTDAs having cm-order spatial resolutions recently have been realized by utilizing pre-pump techniques [5, 6, 7].

More recently, it has been realized that we can use coherence characteristics of spontaneous Brillouin scatterings to achieve the high spatial resolution BOTDRs [8, 9, 10]; then measurements are possible by accessing just one end of the fiber while BOTDAs need two-end access. Double pulse BOTDR (DP-BOTDR) [8] is the first BOTDR that realized a spatial resolution of 20 cm, and needs no major changes in the configuration of the conventional BOTDR. However, the spectrum of the measured Brillouin backscattered light has a plurality of peaks with slightly different intensities, so that a high signal-to-noise ratio is required to accurately measure the BFS. Another high spatial resolution BOTDR is synthetic BOTDR (S-BOTDR) [9]. S-BOTDR uses four types of optical pulse probe generated by superimposing a short-duration and large-amplitude pulse and a long-duration and small-amplitude pulse with quadrature phase shift keying modulation. S-BOTDR synthesizes the Brillouin spectrum from the signals obtained by using the four types of pulse probe. Thus, it can compute the same spectrum as that measured by the conventional BOTDR, achieving precise measurement of BFS and a high spatial resolution. However, S-BOTDR requires the complicated optical modulation technique. In order to solve the above problems, we have proposed phase shift pulse BOTDR (PSP-BOTDR) and have verified its basic principle [10]. However, its spatial resolution characteristic was not satisfactory. In this article, we propose a new way to combine short and long pulses for the probe light of PSP-BOTDR. We report the achievement of 20 cm spatial resolution and observation of 50 MHz spectral width by experiment using the modified probe.

## 2 Principle

Fig. 1(a) shows the signal waveform of the probe pulse light of peak power  $P_0$  proposed in this article for PSP-BOTDR. The probe consists of a long pulse and a short pulse; each pulse duration is  $T_L$  and  $T_S$ , and the pulse interval is  $T_I$ . Figs. 1(a) (1) and 1(a) (2) respectively show the waveforms of 0 phase shift (+) and  $\pi$  phase shift (–) pulses. The difference from the previous report [10] is that this article has reversed the order of the long pulse and the short pulse and has set the interval between the pulses. This modification makes it easier to generate pulses while keeping their intensity the same, as will be described later. The spatial resolution and the Brillouin spectrum width of PSP-BOTDR are determined by  $T_S$  and almost by  $T_L$ , respectively.

The Brillouin backscattered light is detected by an optical heterodyne receiver, and two parts of the signal are sampled with the respective rectangular window functions as shown in Fig. 1(b). The time widths of the intervals of the window functions are the same as the pulse widths of  $T_L$  and  $T_S$ , respectively. When measuring the Brillouin spectrum at the distance  $z$ , as shown in Fig. 1(b), backscattered lights are sampled by  $W_L(t - D + T_L + T_I)$  and  $W_S(t - D + T_L + T_I)$ , where the delay  $D$  from the incidence of the short pulse to the measurement of the backscattered light is given by  $2z/v$  ( $v$  is the speed of light in the optical fiber). Naturally, we cannot achieve high spatial resolution and measure the BFS precisely just by sampling the data with the window functions. However, when we compute cross-correlations of the two sampled data for each measurement using the two types of the pulse probe, and subtract one cross-correlation from the other, we can extract the cross-correlation due to just the backscattered light at the short section ranging from  $z = vD/2$  to  $z = v(D + T_S)/2$ .

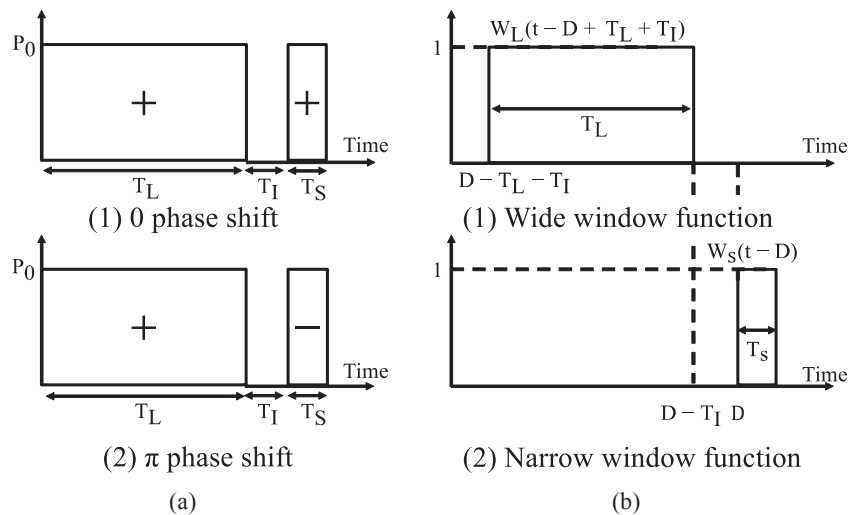


**Fig. 1.** (a) Signal waveform of probe pulses. (b) Two window functions to sample backscattered light.

We define the cross-correlation function  $C_{SL}(\tau)$  and the difference  $\Delta C_{SL}(\tau)$  as follows:

$$C_{SL}^{(\pm)}(\tau) = \left\langle \int b_{WS}^{(\pm)}(t)b_{WL}^{(\pm)}(t + \tau)dt \right\rangle \quad (1)$$

$$\Delta C_{SL}(\tau) = C_{SL}^{(+)}(\tau) - C_{SL}^{(-)}(\tau) \quad (2)$$

where  $\langle \rangle$  denotes ensemble average, and  $b_{WS}(t)$  and  $b_{WL}(t)$  represent backscattered light sampled by the narrow- and the wide-window functions, respectively. In addition, (+) and (–) indicate that the respective parameters are obtained for the pulse probe of Figs. 1(a) (1) and 1(a) (2). Each of the sampled signals includes backscattered light and random noise from different sections. From a statistical point of view, the cross-correlation of random noise is zero. In addition, Brillouin backscattered lights from different sections occur independently, so that the cross-correlation of the backscattered light at different sections is also zero. Therefore, what should be considered in evaluating Eq. (1) is only the cross-correlation between backscattered lights at the same section. In the case of the scattered lights from the section of  $z < vD/2$ , since all scattered lights reach the photodetector before the time  $t = D$ , no backscattered light exist in the time section of  $W_S(t - D)$ . This results in  $b_{WS}(t) = 0$  and thus  $\Delta C_{SL}(\tau) = 0$ . Also, in the case of scattered light from the section of  $z > v(D + T_S)/2$ , whichever probe light in Figs. 1(a) and 1(b) is used,  $b_{WS}(t)$  and  $b_{WL}(t + \tau)$  have the same sign, and as a result, their products  $b_{WS}(t) \cdot b_{WL}(t + \tau)$  for the pulse probe of Figs. 1(a) and 1(b) also become the same, yielding  $\Delta C_{SL}(\tau) = 0$ . In contrast, when the backscattered lights occur at the short section ranging from  $z = vD/2$  to  $z = v(D + T_S)/2$ , the two products have opposite signs with the same magnitude, yielding  $\Delta C_{SL}(\tau) \neq 0$ . From the above discussion, the difference  $\Delta C_{SL}(\tau)$  of Eq. (2) represents the cross-correlation value of the scattering signal from the short section corresponding to the rectangular window function  $W_S(t - D)$  in Fig. 1(b) (2).

In addition, since the Fast Fourier Transform (FFT) of  $\Delta C_{SL}(\tau)$  is given by  $2\langle \text{FFT}[b_{WS}^{(+)}(t)] \cdot \text{FFT}[b_{WL}^{(+)}(t)]^* \rangle$ , its spectrum width becomes narrow, being determined almost by  $\text{FFT}[b_{WL}^{(+)}(t)]$ . It should be noted here that if we use just a short pulse, the spectrum of the Brillouin backscattering has much wider width and it becomes more difficult to estimate the BFS. Therefore, it can be seen that PSP-BOTDR makes it possible to achieve the high spatial resolution and to obtain the narrow Brillouin spectrum width.

### 3 Experimental setup

A measurement system used in the experiment is shown in Fig. 2. The duration of the short pulse  $T_S$  was 2 ns for achieving 20 cm resolution. The duration of the long pulse  $T_L$  was set at 32 ns and the pulse interval  $T_I$  0.5 ns in consideration of the phonon lifetime and the rise time of the signal generator, respectively. The configuration of the experimental system is the same as that of the conventional BOTDR except for the signal processing and the configuration of the pulse probe. The optical pulse with phase shift keying modulation was generated by driving a Mach-Zehnder modulator (MZM) with a bipolar electric pulse in a null bias. In order to generate the beat frequency signal due to the Brillouin backscattered light and the local light near to the center of the frequency band of a balanced photo diode (BPD), the frequency of the probe with a wavelength of 1.55  $\mu\text{m}$  was up-

shifted by a single-side band carrier-suppressed modulator (SSBM). The peak power of the optical probe signal incident on an optical fiber under test was 300 mW. Then, the frequency components of all the Brillouin backscattered lights were simultaneously detected by the BPD. The detected signal was sampled by digital oscilloscope (DO), and FFT using a personal computer was applied to the sampled data for analyzing the Brillouin scattered light spectrum. The waveform of the backscattered light was measured 50,000 times for each of the two pulse probes shown in Fig. 1. We made the fiber under test by splicing two types of single-mode fibers, SMF-1 and SMF-2, as shown in Fig. 2; SMF-1 and SMF-2 differ in BFS by 50 MHz for simulating change in strain of about  $10^{-3}$ .

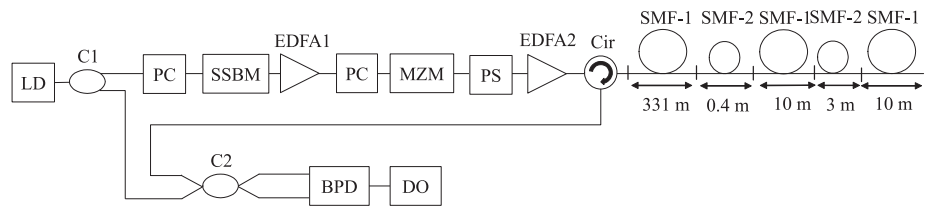


**Fig. 2.** Schematic of experimental setup. LD: laser diode, PC: polarization controller, C: coupler, SSBM: single side band modulator, PS: polarization scrambler, BPD: balanced photo diode, DO: digital oscilloscope, Cir: circulator, EDFA: erbium-doped fiber amplifier, SMF: single-mode fiber

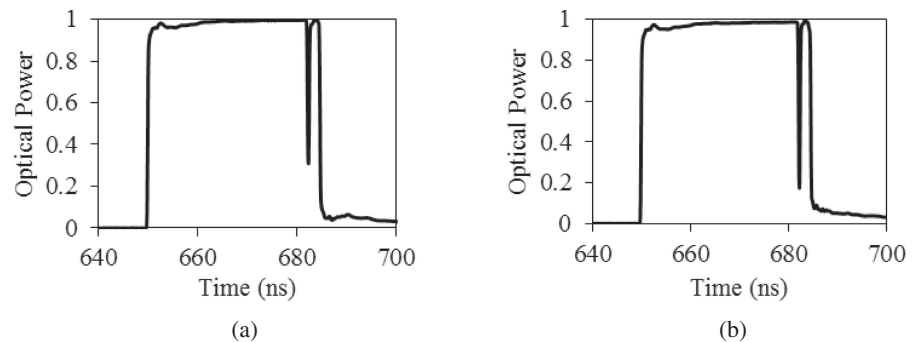
#### 4 Experimental result

Fig. 3 shows the optical intensity signals of the pulse probe incident on the test fiber. In our previous report [10], we placed a short pulse before a long pulse. In this case, fluctuations in optical power occurred during phase shift keying modulation by MZM. Contrary to the previous case, in this article, as shown in Fig. 3, we placed a short pulse after a long pulse and separated the two pulses, thereby suppressing the influence of fluctuation of the optical power. Fig. 3 reveals that the two waveforms of the probe were almost identical. Then, we can expect that the Brillouin scattered light spectrum from the adjacent section will be removed by the subtraction expressed by Eq. (2) and BFS measurement accuracy will be improved.

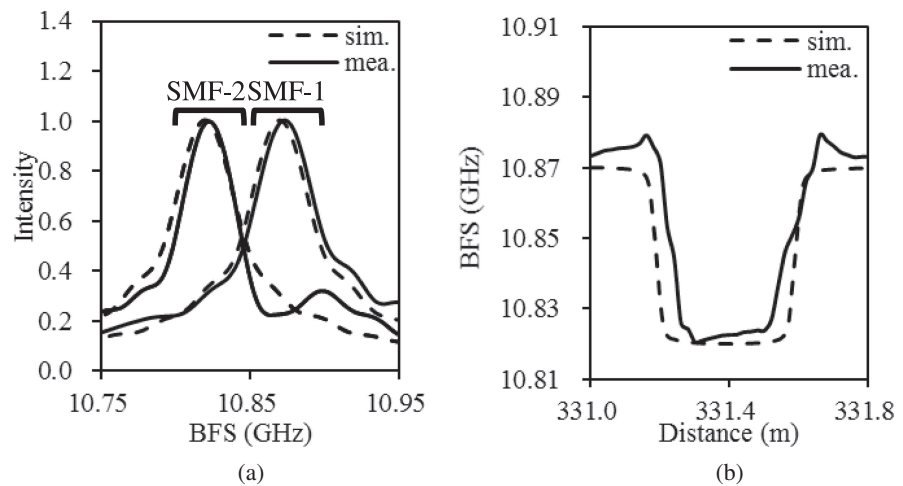
Fig. 4(a) shows the results of measurement and numerical simulation of each Brillouin spectra of the SMF-1 at  $z = 200$  m and the midpoint of 40 cm SMF-2. Both of the measurement and simulation results show that the spectrum of the signal from the adjacent section was reduced to a negligible extent and each spectrum had a narrow width of about 50 MHz.

Fig. 4(b) shows the measurement and the simulation results of Brillouin frequency shift distribution in and around SMF-2 of 40 cm, demonstrating that the frequency transiently changes in the sections of 20 cm or less on the boundaries between SMF-1 and SMF-2. Therefore, we have confirmed that the spatial resolution of 20 cm was truly achieved. We also evaluated the standard deviation of the BFS of 40 cm SMF-2 at 1.08 MHz, which corresponds to a strain accuracy of about  $2 \times 10^{-5}$ . Fig. 4(b) exhibited slight difference between the simulation and the

measurement. This reason is probably that we did not take account of optical-receiver noise for the simulation and that a slight difference still remained in the waveforms of the two probes.



**Fig. 3.** Pulse probe incident on the test fiber. (a) 0 phase shift. (b)  $\pi$  phase shift.



**Fig. 4.** Measurements and simulations. (a) Brillouin spectrum. (b) BFS distribution.

## 5 Conclusion

We have proposed PSP-BOTDR using a new formation of pulsed probe; a short pulse has been placed after a long pulse with a slight separation. The new configuration has allowed us to generate two types of phase-modulated probe signals with approximately the same intensity-waveform. This results in reducing the backscattered light from the adjacent section, which was a problem in the previous PSP-BOTDR. Furthermore, we have measured the BFS distribution with a high spatial resolution of 20 cm along the test optical fiber of 354.4 m and with a frequency accuracy of 1.08 MHz. In addition, we have evaluated the Brillouin spectrum width at 50 MHz that is near to that measured for continuous wave probe.